Published OnlineFirst April 14, 2015; DOI: 10.1158/2159-8290.CD-14-1096

RESEARCH BRIEF

Germline Mutations in the *CDKN2B* Tumor Suppressor Gene Predispose to Renal Cell Carcinoma

Mariam Jafri[1,2], Naomi C. Wake[1], David B. Ascher[3], Douglas E.V. Pires[3], Dean Gentle[1], Mark R. Morris[1,4], Eleanor Rattenberry[1,5], Michael A. Simpson[6], Richard C. Trembath[6,7], Astrid Weber[8], Emma R. Woodward[1,5], Alan Donaldson[9], Tom L. Blundell[3], Farida Latif[1], and Eamonn R. Maher[1,10]

ABSTRACT Familial renal cell carcinoma (RCC) is genetically heterogeneous and may be caused by mutations in multiple genes, including *VHL*, *MET*, *SDHB*, *FH*, *FLCN*, *PTEN*, and *BAP1*. However, most individuals with inherited RCC do not have a detectable germline mutation. To identify novel inherited RCC genes, we undertook exome resequencing studies in a familial RCC kindred and identified a *CDKN2B* nonsense mutation that segregated with familial RCC status. Targeted resequencing of *CDKN2B* in individuals ($n = 82$) with features of inherited RCC then revealed three candidate *CDKN2B* missense mutations (p.Pro40Thr, p.Ala23Glu, and p.Asp86Asn). *In silico* analysis of the three-dimensional structures indicated that each missense substitution was likely pathogenic through reduced stability of the mutant or reduced affinity for cyclin-dependent kinases 4 and 6, and *in vitro* studies demonstrated that each of the mutations impaired CDKN2B-induced suppression of proliferation in an RCC cell line. These findings identify germline *CDKN2B* mutations as a novel cause of familial RCC.

SIGNIFICANCE: Germline loss-of-function *CDKN2B* mutations were identified in a subset of patients with features of inherited RCC. Detection of germline *CDKN2B* mutations will have an impact on familial cancer screening and might prove to influence the management of disseminated disease. *Cancer Discov; 5(7); 723–9. ©2015 AACR.*

INTRODUCTION

The identification of the genetic basis for familial cancer syndromes can provide important insights into the molecular mechanisms of familial and sporadic tumorigenesis. Furthermore, improved understanding of the molecular factors involved in tumorigenesis has provided a basis for the rational development of targeted therapies. This is exemplified in inherited renal cell carcinoma (RCC; MIM#144700) in which the identification of mutations in the *VHL* tumor suppressor

[1]Medical and Molecular Genetics, School of Clinical and Experimental Medicine, College of Medical and Dental Sciences, University of Birmingham, Birmingham, United Kingdom. [2]Department of Oncology, University Hospital Birmingham Foundation Trust, Birmingham, United Kingdom. [3]Department of Biochemistry, University of Cambridge, Cambridge, United Kingdom. [4]School of Applied Sciences, University of Wolverhampton, Wolverhampton, United Kingdom. [5]West Midlands Region Genetics Service, Birmingham Women's Hospital, Birmingham, United Kingdom. [6]Division of Genetics and Molecular Medicine, King's College London School of Medicine, Guy's Hospital, London, United Kingdom. [7]Queen Mary University of London, Barts and The London School of Medicine and Dentistry, London, United Kingdom. [8]Royal Liverpool Children's Hospital, Liverpool, United Kingdom. [9]Department of Clinical Genetics, University Hospital Bristol NHS Trust, St. Michael's Hospital, Bristol, United Kingdom. [10]Department of Medical Genetics, University of Cambridge and NIHR Cambridge Biomedical Research Centre, Cambridge, United Kingdom.

Current address for D.E.V. Pires: Centro de Pesquisas René Rachou, Fundação Oswaldo Cruz, Belo Horizonte, Brazil.

Corresponding Author: Eamonn R. Maher, University of Cambridge, Box 238, Cambridge Biomedical Campus, Cambridge CB2 2QQ, UK. Phone: 01223-746715; Fax: 01223-746777; E-mail: erm1000@medschl.cam.ac.uk

doi: 10.1158/2159-8290.CD-14-1096

Published OnlineFirst April 14, 2015; DOI: 10.1158/2159-8290.CD-14-1096

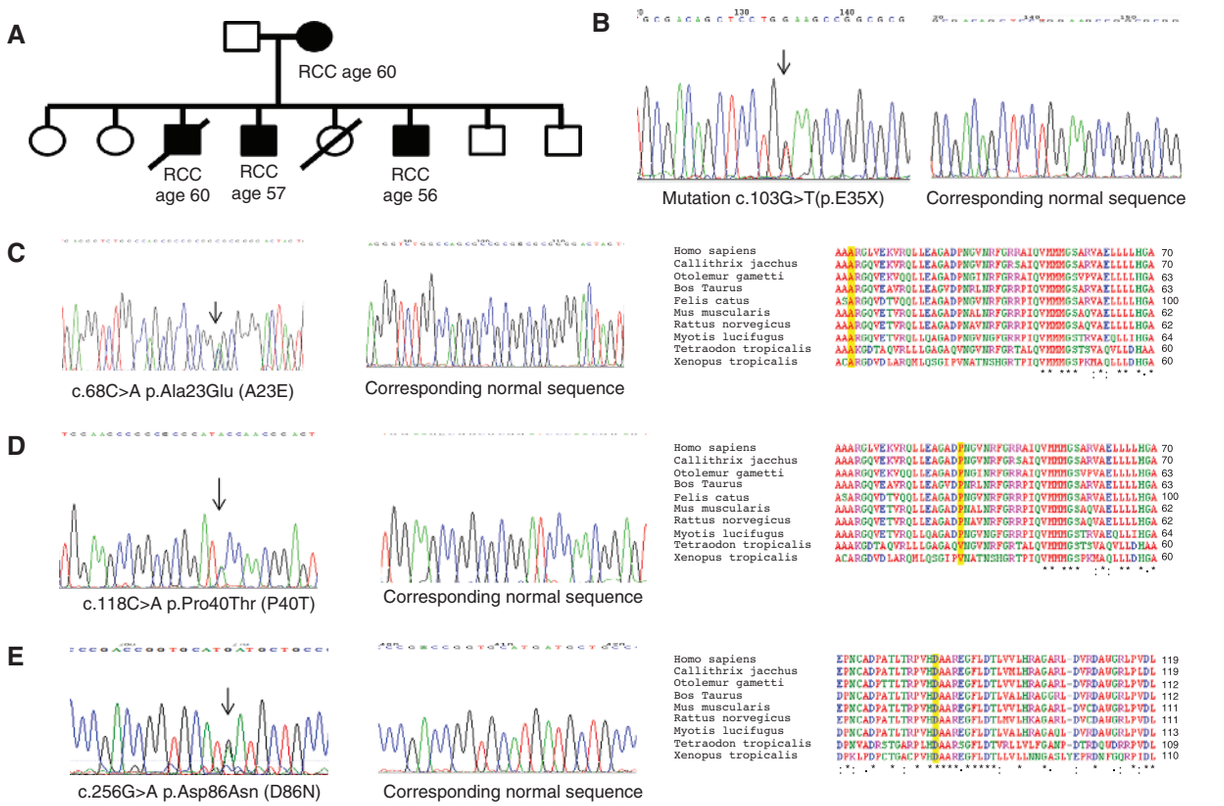

Figure 1. **A,** family pedigree for familial RCC kindred in which exome sequencing was performed. **B,** electropherogram showing heterozygous nonsense mutation (c.103G>T). **C,** electropherogram showing heterozygous missense mutation c.68C>A p.Ala23Glu (A23E) and evolutionary conservation of residue; **D,** electropherogram showing heterozygous missense mutation c. 118C>A p.Pro40Thr (P40T) and evolutionary conservation of residue; **E,** electropherogram showing heterozygous missense mutation. c.256G>A p.Asp86Asn (D86N) and evolutionary conservation of residue.

gene (TSG) as the cause of von Hippel–Lindau (VHL) disease (MIM#193300) led to the recognition that the *VHL* TSG is somatically inactivated in the majority of sporadic clear-cell RCC. Subsequently, elucidation of the role of the *VHL* gene product in the regulation of hypoxia response pathways enabled the development of novel targeted treatments that have revolutionized the clinical management of RCC (1).

About 3% of all cases of RCC occur in individuals with familial RCC (2). A number of genetic mechanisms have been implicated in RCC predisposition. Thus, genome-wide association studies have identified several common genetic variants that predispose to RCC, and at least two loci are linked to pVHL-regulated hypoxic gene response pathways [at 2p21 (rs11894252) and 11q13.3 (rs7105934) close to *EPAS1* (*HIF2A*) and *CCND1* (Cyclin D1), respectively; ref. 3]. In familial RCC, in addition to *VHL*, germline mutations in *MET*, *FLCN*, *FH*, *SDHB*, *PTEN*, and *BAP1* have all been associated with inherited RCC [2 (and references within), 4–6]. Constitutional translocations, particularly involving chromosome 3, can also cause inherited RCC (7). However, overall less than 20% of patients with features of nonsyndromic inherited RCC have a detectable mutation in a known familial RCC gene (2, 4–6, 8, 9). To identify novel inherited RCC genes, we undertook exome sequencing and targeted resequencing studies in individuals with features of inherited RCC and no detectable mutation in known RCC predisposition genes.

RESULTS

Identification of *CDKN2B* Mutations in Inherited RCC

Analysis of exome resequencing in a male proband diagnosed with familial clear-cell RCC (see Fig. 1A) at age 57 years revealed no candidate mutations in RCC predisposition genes (*VHL*, *SDHB*, *FLCN*, *FH*, *PTEN*, or *BAP1*). Further bioinformatic analysis was undertaken for the presence of pathogenic mutations in genes linked to cancer. A candidate nonsense mutation in *CDKN2B* was highlighted for further investigation, and the *CDKN2B* c.103G>T (p.Glu35Stop) mutation was confirmed by Sanger sequencing (see Fig. 1B). Two of his eight siblings had been diagnosed with clear-cell RCC (two brothers diagnosed at ages 56 and 60 years, respectively), and his mother had been diagnosed with RCC at age 60 years. DNA was available from four living relatives, and family genotyping studies demonstrated the c.103G>T *CDKN2B* nonsense mutation was present in the only living sibling affected by RCC, but not in three unaffected siblings (Fig. 1A). The c.103G>T *CDKN2B* nonsense mutation was not previously reported in publicly available large exome/genome sequencing sets comprising >13,000 *CDKN2B* alleles (0/1,092 sample chromosomes in 1,000 genomes; ref. 10; and 0 of >6,000 samples in the NHLBI Exome Variant Server; ref. 11). In addition, no other *CDKN2B* truncating mutations were reported in the latter set of >12,000 *CDKN2B* alleles.

Published OnlineFirst April 14, 2015; DOI: 10.1158/2159-8290.CD-14-1096

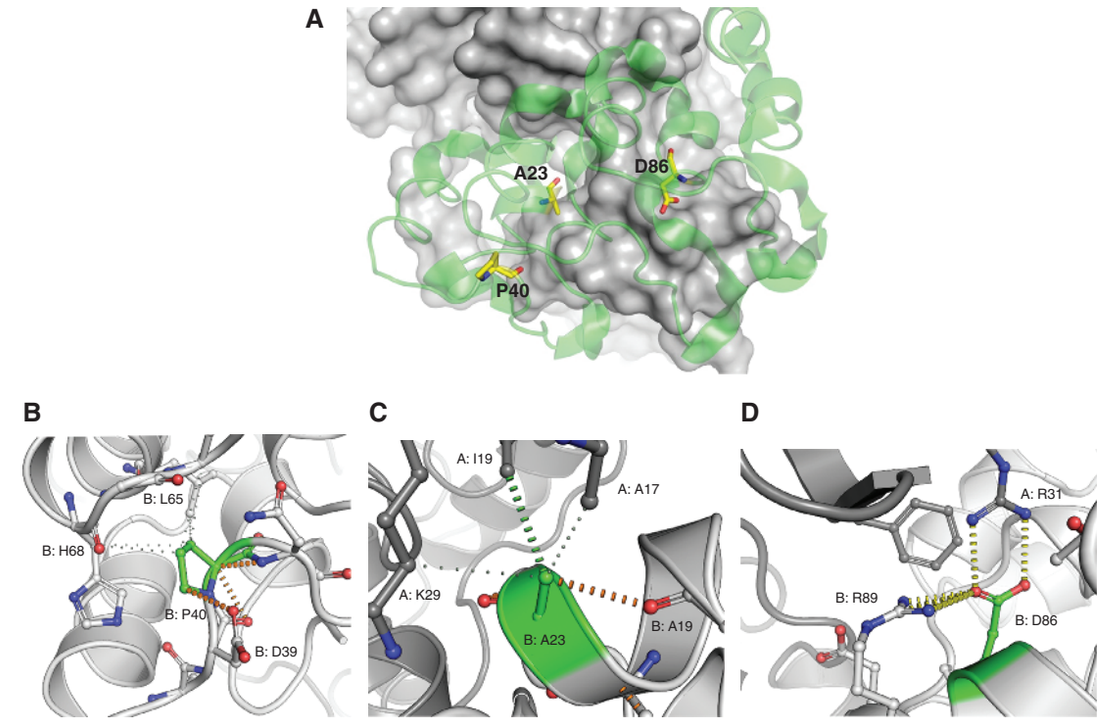

Figure 2. Structural analysis of the interaction network of variant residues in CDKN2B (for the wild-type CDKN2B–CDK6). Ionic interactions and hydrogen bonds are depicted as yellow dashes, hydrophobic interactions are presented in green, and weak polar interactions are presented in orange. **A,** overview: atoms from CDKN2B and CDK6 are shown in light green and dark gray, respectively; (**B**) p.Pro40, (**C**) p.Ala23, and (**D**) p.Asp86. CDK, cyclin-dependent kinase.

To further investigate the potential role of *CDKN2B* mutations in inherited renal cancer, mutation screening was performed in 50 individuals with features of nonsyndromic inherited RCC [either familial RCC ($n = 37$) or multiple RCC aged <50 years ($n = 13$)], and three candidate missense mutations were detected (Fig. 1C–E). A rare sequence variant (c.256G>A) predicted to cause a pathogenic missense substitution, p.Asp86Asn, was detected in a proband who was diagnosed with clear-cell RCC at age 35 years. No other family members (her mother had died from RCC) were available for testing. In addition, a novel candidate mutation [c.118C>A (p.Pro40Thr)] was identified in an individual who developed bilateral RCC at age 42 years. No other family members were available for testing. Mutation analysis of *CDKN2B* in a cohort of 34 individuals with features of possible inherited RCC (familial RCC, multicentric RCC, or young onset RCC) revealed candidate heterozygous missense substitutions [c. 68C>A (p.Ala23Glu)] in one case. Two of the three candidate *CDKN2B* missense mutations (p.Ala23Glu and p.Pro40Thr) were absent from publicly available large exome/genome sequencing sets comprising >12,000 *CDKN2B* alleles, and the p.Asp86Asn variant occurred with a frequency of <1 in 200 individuals (11). All three substitutions occurred at evolutionarily conserved residues (see Fig. 1C–E) and were predicted to be pathogenic by Polyphen and SIFT algorithms (12, 13).

Structural Predictions

To understand the potential impact of the mutations on CDKN2B, the mutations were analyzed in the context of the apo (unbound) structure, and in complex with cyclin-dependent kinases (CDK) 4 or 6. The overall structure of CDKN2B is very similar to CDKN2D and is expected to bind through its concave face to the cleft between the N- and C-terminal domains of CDK4 and CDK6. Binding of CDKN2B prevents productive binding of ATP to the CDKs, and potentially inhibiting movement of the PLSTIRE helix to its active conformation (14).

The three variants identified were spread across the protein (Fig. 2A), with p.Ala23 and p.Asp86 located close to the surface, and along the interface with CDK4 and CDK6, whereas p.Pro40 is a buried residue distal to the interaction interface. CDKN2B p.Pro40 is located on a hydrogen-bonded turn leading into the sheet of the first ankyrin repeat and forming interactions with helices in the first and second ankyrin repeats (Fig. 2B). The first two ankyrin repeats mediate the majority of the interactions with the CDKs (14). Mutation to threonine relaxes this loop, altering the packing of the helices and the overall stability of CDKN2B, as predicted by mCSM and DUET (Table 1).

CDKN2B p.Ala23 is located on an α-helix at the periphery of the interface among CDKN2B and CDK4 and CDK6, where it makes a series of inter- and intramolecular weak hydrophobic interactions (Fig. 2C). This space is not sufficient to accommodate the larger, charged glutamate residue in the mutant, leading to a reduced affinity for the CDKs as predicted by mCSM-PPI (Table 1). CDKN2B p.Asp86 is also located on an α-helix and makes strong intermolecular ionic/hydrogen bonds with CDK4 and CDK6 (Fig. 2D). In the variant, the asparagine side chain is unable to make these

Published OnlineFirst April 14, 2015; DOI: 10.1158/2159-8290.CD-14-1096

Table 1. Predicted effects of mutations upon CDKN2B stability and protein interactions

Variant	Secondary structure	Solvent accessibility	CDKN2B stability—mCSM (ΔΔG kcal/mol)	CDKN2B stability—DUET (ΔΔG kcal/mol)	CDKN2B–CDK4 affinity (ΔΔG kcal/mol)	CDKN2B–CDK6 affinity (ΔΔG kcal/mol)
p.Pro40Thr	h-bonded turn	5.3% (buried)	−1.8[a]	−1.9[a]	−0.6	−0.6
p.Asp86Asn	α-helix	27.1% (partially accessible)	−0.9	−0.8	−1.8[a]	−2.2[a]
p.Ala23Glu	α-helix	44.9% (partially accessible)	−1.3[a]	−1.1[a]	−2.5[a]	−1.0[a]

[a]Highly destabilizing.

interactions, leading to a significant reduction in affinity as predicted by mCSM-PPI (Table 1).

Functional Effects of Germline *CDKN2B* Variants

To evaluate the pathogenicity of the candidate germline mutations detected in inherited RCC cases, we undertook *in vitro* studies of growth suppressor activity. Thus, the effects on growth of the two RCC cell lines were compared for (i) wild-type *CDKN2B*, (ii) vector only [empty vector (EV)], and (iii) the three candidate missense substitutions: p.Pro40Thr, p.Ala23Glu, and p.Asp86Asn. Initially, the effects of transfecting a vector expressing wild-type *CDKN2B* and an EV into the SKRC47 (wild-type *VHL*) and KTCL26 (VHL-null) RCC cell lines were compared with the colony formation assay. For both cell lines, there were significantly fewer colonies after transfection with wild-type *CDKN2B* than with the EV control. The effects of the three candidate missense mutations (p.Pro40Thr, p.Ala23Glu, and p.Asp86Asn) were then studied, and each missense mutation impaired *in vitro* growth suppressor activity of CDKN2B (Fig. 3).

DISCUSSION

We identified germline-inactivating *CDKN2B* mutations in approximately 5% (95% confidence interval, 0.21%–9.43%) of patients with features of nonsyndromic inherited RCC analyzed. Thus, the frequency of germline *CDKN2B* mutations is approximately similar to that which can be attributed to germline *FLCN* and *SDHB* mutations (8, 9) but larger than that accounted for by germline *BAP1* mutations (5, 6). These mutations lead to the deregulation of CDK4 and CDK6 by CDKN2B, by altering the binding interfaces or overall stability of CDKN2B. The identification of *CDKN2B* as an inherited RCC gene will facilitate the diagnosis and management of this disorder. In addition to a nonsense mutation that segregated with RCC in familial RCC kindred, we identified three rare missense mutations in individuals with features of inherited RCC. Two of these missense mutations were novel, but one (NM_004936 c.256G>A p.Asp86Asn) had previously been reported in a patient with parathyroid adenoma and in a patient with a metastatic pancreatic endocrine tumor (15, 16). The p.Asp86Asn substitution occurs at a highly conserved residue and has an allele frequency of approximately 0.2% in Single Nucleotide Polymorphism database (dbSNP) build 137 (17), and, consistent with the *in silico* structural predictions reported here, Costa-Guda and colleagues (15) demonstrated that the p.Asp86Asn substitution inhibited binding of CDKN2B/p15 to CDK6.

CDKN2B encodes the $p15^{INK4B}$ protein, which binds to and inhibits CDK4 and CDK6 (18). In the absence of CDKN2B, CDK4- and CDK6-dependent phosphorylation of pRb inhibits the interaction between pRb and E2F and promotes cell growth. Overexpression of $p15^{INK4B}$ causes cell-cycle arrest in G_1 phase and redistribution of CDK4 from cyclin D–CDK4 complexes to CDK4–$p15^{INK4B}$ complexes, leading to degradation of unbound cyclin D by the ubiquitin-dependent proteasome degradation pathway (18). Interestingly, cyclin D1 is a downstream target of pVHL, inactivation of the *VHL* TSG is associated with HIF2-dependent upregulation of cyclin D1 (19), and genome-wide association studies identified genetic variation linked to *CCND1* expression with RCC susceptibility (3). The *CDKN2B* gene maps close to the *CDKN2A* locus that encodes two tumor suppressor proteins (p16INK4a and p14ARF), and many deletions found in human cancer encompass both *CDKN2B* and *CDKN2A*. However, experiments in mice demonstrated that *Cdkn2b* also possesses critical tumor suppressor activity (20). Though somatic *CDKN2B* mutations are uncommon in human neoplasia, somatic inactivation of *CDKN2B* by allele loss and/or promoter hypermethylation has been reported in a variety of human cancers, most notably hematologic neoplasms, including leukemia, lymphoma, and myelodysplastic syndrome (21). Cytogenetic studies have identified chromosome 9p deletions in approximately 15% of clear-cell RCC, array-based studies of copy-number abnormalities have confirmed that the 9p critical region contains the *CDKN2A/CDKN2B* loci, and Girgis and colleagues (22) found that a subset of RCC exhibited hypermethylation of *CDKN2A* and *CDKN2B* (13% and 21%, respectively).

Previously, *CDKN2B* mutations have been linked to predisposition to endocrine tumors (15, 16, 23). Thus, in addition to p.Asp86Asn mutation that was reported in individuals with a parathyroid adenoma (wild-type allele loss was detected in the tumor tissue) and metastatic pancreatic endocrine tumor (15, 16), two further missense mutations (p.Asn41Asp and p.Leu64Arg) were reported in patients with suspected multiple endocrine neoplasia: one with primary hyperparathyroidism (3 parathyroid tumors), skin schwannoma, meningioma, and liver hemangioma, and one with primary hyperparathyroidism (3 parathyroid tumors), Zollinger–Ellison syndrome, adrenal

Published OnlineFirst April 14, 2015; DOI: 10.1158/2159-8290.CD-14-1096

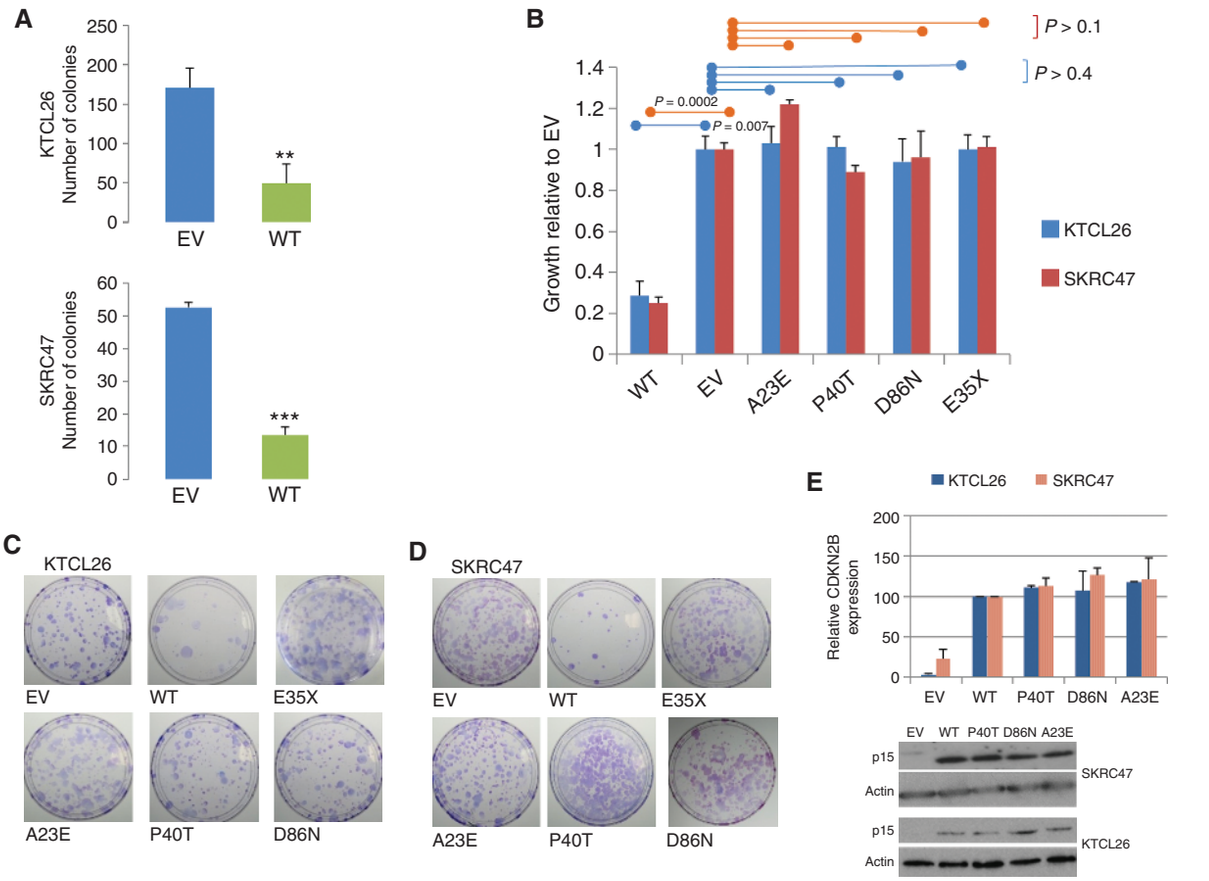

Figure 3. Functional evaluation of *CDKN2B* mutations using colony formation assays. **A,** comparison of EV and wild-type (WT) *CDKN2B* expression in KTCL26 and SKRC47 RCC cell lines. Transfection with wild-type *CDKN2B* significantly reduced the number of colonies formed ($t = 3.936$, degree of freedom = 6, $P = 0.007$ and $t = 18.2$, $P = 0.0002$, respectively). **, $P = 0.007$; ***, $P = 0.0002$. **B,** comparison of growth suppression (by colony formation assay) of EV, wild-type *CDKN2B*, and three candidate missense mutations [p.Pro40Thr (P40T), p.Ala23Glu (A23E), and p.Asp86Asn (D86N)] in KTCL26 RCC (VHL-null) and SKRC47 (VHL-positive) cell lines. There were no statistically significant differences ($P > 0.4$ for KTCL26 and $P > 0.1$ for SKRC47) between the number of colonies in cell lines transfected with EV compared with those transfected with missense mutants containing variants. **C** and **D,** representative colony formation assay plates stained using crystal violet from colonies derived from KTCL26 (VHL-null) and SKRC47 (VHL-positive) cell lines transfected with either wild-type *CDKN2B*, EV, or vector containing the following variants: p.Pro40Thr (P40T), p.Ala23Glu (A23E), and p.Asp86Asn (D86N). **E,** representative CDKN2B expression levels for the colony formation assays. Expression levels for the three missense mutations were comparable to that for wild-type protein expression [data represents the mean (of 3 experiments) with error bars representing the SE].

mass, and prostate cancer. Both p.Asn41Asp and p.Leu64Arg substitutions impaired binding to CDK6 (23). The finding of multiple phenotypes with mutations in a single gene is not uncommon and may reflect variable modes of ascertainment and/or genotype–phenotype correlations. Thus, germline *BAP1* mutations were initially described in association with uveal melanoma, mesothelioma, and other tumors before being recognized as a cause of familial RCC (5, 6), and, recently, mutations in *FH* were detected in individuals with pheochromocytoma/paraganglioma without features of hereditary leiomyomatosis–RCC (Reed syndrome; refs. 24, 25). In our study, none of the confirmed *CDKN2B* mutation carriers were known to have a nonrenal neoplasm, but further studies will define the full range of tumor types associated with *CDKN2B* mutations. It is interesting to note that germline mutations in *CDC73* (cell division cycle 73) predispose to both parathyroid and renal tumors (26), and the *CDC73* gene product (parafibromin) has been reported to repress cyclin D1 expression and induce cell-cycle arrest (27).

As the inventory of genetic and epigenetic changes described in RCC enlarges, the challenge of differentiating "driver" and "passenger" events increases. Identification of the genetic basis of inherited cancer provides a powerful strategy for highlighting key pathways in oncogenesis. Thus, though the *VHL* TSG is frequently somatically inactivated in sporadic RCC, other inherited RCC genes, such as *FH*, *FLCN*, and *SDHB*, are infrequently implicated in RCC but, like pVHL, have been linked to regulation of hypoxic gene response pathways. The finding that germline *CDKN2B* mutations predispose to RCC is consistent with the observation that *VHL* inactivation is associated with disordered cell-cycle regulation and provides a basis for investigating the role of cell-cycle inhibitors (e.g., palbociclib) for the treatment of advanced RCC—particularly in patients with germline *CDKN2B* mutations. Thus, inclusion of *CDKN2B* mutation analysis in the routine investigation of individuals could facilitate the management of both affected individuals and their at-risk relatives.

Published OnlineFirst April 14, 2015; DOI: 10.1158/2159-8290.CD-14-1096

METHODS

Patients

Whole-exome sequencing was undertaken in the proband from a kindred with familial RCC (see Fig. 1A). Following the identification of a candidate germline *CDKN2B* mutation in the proband, mutation analysis of *CDKN2B* was performed in other family members and in a further 50 unrelated probands with (i) a diagnosis of RCC and a family history of one or more close relatives with a history of RCC (n = 37, 19 males and 18 females; mean age, 52.9 years; range, 29–71 years) or (ii) two or more primary RCC before age 50 years (n = 13, 7 males and 6 females; mean age, 41 years; range, 17–49 years). In addition, a further 32 DNA samples were tested from an anonymized cohort of individuals with evidence of possible inherited predisposition to RCC [i.e., a diagnosis of RCC plus one of (i) positive family history or (ii) multiple primary RCC or (iii) early onset RCC (<40 years)]. All subjects gave consent for genetic studies; the investigations were approved by the South Birmingham Research Ethics committee and were conducted in accordance with the Declaration of Helsinki.

Molecular Genetic Analysis

Exome resequencing was performed at the Biomedical Research Centre at King's College London as described previously (28). Briefly, after extraction of DNA from peripheral blood lymphocytes using standard techniques, exon capture was performed using the Agilent Sure Select All Exon 50 Mb Target Enrichment System. The Illumina Analyser IIA with 76 base paired ends and reads was used for sequencing, and the depth of sequence coverage was calculated using the BedTools software package (29). Sequence alignment, identification of SNPs, and small deletions were identified by the SAMTools software package (30). The ANNOVAR software package (31) was used to filter data for variants identified in dbSNP and common SNPs in the 1,000 genomes data. Furthermore, data were compared with 250 control exomes sequenced by the same method.

Sanger Sequencing

Sanger sequencing was performed using standard techniques. The following primer pairs were used:

CDKN2B exon 1: 5′-AAGAGTGTCGTTAAGTTTACG-3′ and 5′-ACATCGGCGATCTAGGTTCCA-3′,
CDKN2B exon 2: 5′-TGAGTATAACCTGAAGGTGG-3′ and 5′-GGGTGGGAAATTGGGTAAG-3′.

The following conditions were used: (i) 95°C for 5 minutes, (ii) 95°C for 45 seconds, (iii) 58°C for 45 seconds, decreasing by 1°C per cycle, (iv) repeat steps (i) to (iii) for 4 cycles, (v) 95°C for 45 seconds, (vi) 54°C for 45 seconds, (vii) 72°C for 45 seconds, (viii) repeat (v) to (vii) 30 times, (viii) incubate at 72°C for 5 minutes.

Colony Formation Assays

The *CDKN2B* clone was obtained from Cambridge Bioscience (True ORF Gold RC204895). The sequence of the clone was confirmed by direct sequencing. Site-directed mutagenesis was performed on the *CDKN2B* clone using the Quik Change II Site Directed Mutagenesis Kit (Stratagene; obtained from Agilent Technologies; primer details available on request). Mutant plasmids were sequenced in order to confirm the presence of the variant. Silver competent cells (Bioline) were transformed with mutant plasmid, and the plasmid was amplified to a stock concentration of 1 μg/μL using the Endotoxin-Free Maxi Spin Kit (Qiagen). The *VHL*-null cell line KTCL26 and the *VHL*–wild-type cell line SKRC47 were plated at a density of 6×10^4/mL in 6-well plates on day 1. Transfection was carried out on day 2 using 2 μg plasmid diluted in 200 μL of OptiMem (Gibco) and 6 μL of Fugene HD (Promega) per well. A serial dilution was performed in KTCL26 cells treated with EV and wild-type using the following dilutions: undiluted, 1:5, 1:10, 1:20. Dilutions (1:5) were used for subsequent experiments. The KTCL26 and SKRC47 cell lines were obtained from a collaborator prior to 2006, and no authentication was performed apart from confirming a *VHL* mutation [(c.370 C>T) p.Gln124Stop] in KTCL26 and the absence of a *VHL* mutation in SKRC47 (32).

Molecular Modeling

Models of CDKN2B in complex with CDK4 or CDK6 were based on the X-ray crystal structure of CDK6 in complex with CDKN2D (PDB code: 1BLX; ref. 14) and generated using Modeller (33) and MacroModel (Schrodinger). The models were then minimized using the MMF94s forcefield in Sybyl-X 2.1.1 (Certara L.P.). The resulting models were then aligned to the nuclear magnetic resonance (NMR) structure of CDKN2B (PDB code 1D9S; ref. 34) and showed minimal variation in the overall structure [root mean square difference (r.m.s.d) over Cαs of 1.6 Å]. The difference is mainly due to a small long-range bending of the molecule. The model of CDK4 was also compared with the CDK4 apo structure (PDB code: 3G33. r.m.s.d over Cαs of 1.1 Å). The effects of the mutations on the stability of CDKN2B were analyzed by mCSM (35) and DUET (36) using both the models and the apo NMR structure (PDB code: 1D9S). The effects of the mutations on the affinity of CDKN2B for CDK4 and CDK6 were analyzed by mCSM-PPI (35) using the models of the complexes. DUET and mCSM are novel machine-learning algorithms that use the three-dimensional structure in order to quantitatively predict the effects of point mutations on protein stability and protein–protein and protein–nucleic acid affinities.

Statistical Analysis

T tests were performed using SPSS Statistics 21 (IBM software). To allow for multiple comparisons in Fig. 3 (wild-type and four mutants), a P value of <0.01 was taken to be statistically significant.

Disclosure of Potential Conflicts of Interest

T.L. Blundell is a deputy chair trustee at the Institute of Cancer Research; President and Chair of the Science Council; and a consultant/advisory board member for Astex Therapeutics and BBSRC; has received a commercial research grant from UCB Celltech; and has provided expert testimony for Isogenica, Pfizer, and Syntaxin. No potential conflicts of interest were disclosed by the other authors.

Authors' Contributions

Conception and design: M. Jafri, E.R. Woodward, F. Latif, E.R. Maher
Development of methodology: M. Jafri, N.C. Wake, M.R. Morris, M.A. Simpson, R.C. Trembath, T.L. Blundell
Acquisition of data (provided animals, acquired and managed patients, provided facilities, etc.): M. Jafri, E. Rattenberry, M.A. Simpson, R.C. Trembath, A. Weber, E.R. Woodward, A. Donaldson, E.R. Maher
Analysis and interpretation of data (e.g., statistical analysis, biostatistics, computational analysis): M. Jafri, N.C. Wake, D.B. Ascher, D.E.V. Pires, M.R. Morris, E. Rattenberry, M.A. Simpson, T.L. Blundell
Writing, review, and/or revision of the manuscript: M. Jafri, D.B. Ascher, D.E.V. Pires, M.R. Morris, E.R. Woodward, F. Latif, E.R. Maher
Administrative, technical, or material support (i.e., reporting or organizing data, constructing databases): M. Jafri, D. Gentle
Study supervision: E.R. Maher

Acknowledgments

The authors thank the patients, families, and referring clinicians for their assistance.

Grant Support

M. Jafri is in receipt of a Medical Research Council Clinical Research Fellowship. D.B. Ascher is supported by a National Health and Medical Research Council CJ Martin Fellowship. D.E.V. Pires is supported by the Conselho Nacional de Desenvolvimento Científico e Tecnológico (CNPq)—Brazil. M.A. Simpson thanks the National Institutes for Health Research (NIHR) Biomedical Research Centre based at Guy's and St. Thomas' NHS Foundation Trust and King's College London for financial support. E.R. Maher thanks the Association for International Cancer Research (AICR; now Worldwide Cancer Research), The Eveson Charitable Trust, and the NIHR Biomedical Research Centre based at Cambridge for financial support.

The costs of publication of this article were defrayed in part by the payment of page charges. This article must therefore be hereby marked *advertisement* in accordance with 18 U.S.C. Section 1734 solely to indicate this fact.

Received September 18, 2014; revised April 1, 2015; accepted April 9, 2015; published OnlineFirst April 14, 2015.

REFERENCES

1. Banegas MP, Harlan LC, Mann B, Yabroff KR. Renal cell cancer: a shift in approaches for treatment of advanced disease in the United States. J Natl Compr Canc Netw 2014;12:1271–9.
2. Maher ER. Genetics of familial renal cancers. Nephron Exp Nephrol 2011;118:e21–6.
3. Purdue MP, Johansson M, Zelenika D, Toro JR, Scelo G, Moore LE, et al. Genome-wide association study of renal cell carcinoma identifies two susceptibility loci on 2p21 and 11q13.3. Nat Genet 2011;43:60–5.
4. Mester JL, Zhou M, Prescott N, Eng C. Papillary renal cell carcinoma is associated with PTEN hamartoma tumor syndrome. Urology 2012;79:1187.e1–7.
5. Farley MN, Schmidt LS, Mester JL, Pena-Llopis S, Pavia-Jimenez A, Christie A, et al. Germline BAP1 mutation predisposes to familial clear-cell renal cell carcinoma. Mol Cancer Res 2013;11:1061–71.
6. Popova T, Hebert L, Jacquemin V, Gad S, Caux-Moncoutier V, Dubois-d'Enghien C, et al. Germline BAP1 mutations predispose to renal cell carcinomas. Am J Hum Genet 2013;92:974–80.
7. Woodward ER, Skytte A-B, Cruger DG, Maher ER. Population-based survey of cancer risks in chromosome 3 translocation carriers. Genes Chromosomes Cancer 2010;49:52–8.
8. Woodward ER, Ricketts C, Killick P, Gad S, Morris MR, Kavalier F, et al. Familial Non-VHL clear cell (conventional) renal cell carcinoma: clinical features, segregation analysis, and mutation analysis of FLCN. Clin Cancer Res 2008;14:5925–30.
9. Ricketts C, Woodward ER, Killick P, Morris MR, Astuti D, Latif F, et al. Germline SDHB mutations and familial renal cell carcinoma. J Natl Cancer Inst 2008;100:1260–2.
10. 1000 Genomes Project Consortium, Abecasis GR, Auton A, Brooks LD, DePristo MA, Durbin RM, et al. An integrated map of genetic variation from 1,092 human genomes. Nature 2012:491:56–65.
11. NHLBI Exome Variant Server [homepage on the Internet]. Available from: <http://evs.gs.washington.edu/EVS/>. Accessed 8/28/2014.
12. Adzhubei IA, Schmidt S, Peshkin L, Ramensky VE, Gerasimova A, Bork P, et al. A method and server for predicting damaging missense mutations. Nat Methods 2010;7:248–9.
13. Kumar P, Henikoff S, Ng PC. Predicting the effects of coding non-synonymous variants on protein function using the SIFT algorithm. Nat Protoc 2009;4:1073–81.
14. Brotherton DH, Dhanaraj V, Wick S, Brizuela L, Domaille PJ, Volyanik E, et al. Crystal structure of the complex of the cyclin D-dependent kinase Cdk6 bound to the cell-cycle inhibitor p19INK4d. Nature 1998;395:244–50.
15. Costa-Guda JSC, Parekh VI, Agarwal SK. Germline and somatic mutations in cyclin-dependent kinase inhibitor genes CDKN1A, CDKN2B, and CDKN2C in sporadic parathyroid adenomas. Hormones Cancer 2013;4:301–7.
16. Lindberg D, Åkerström G, Westin G. Evaluation of CDKN2C/p18, CDKN1B/p27 and CDKN2B/p15 mRNA expression, and CpG methylation status in sporadic and MEN1-associated pancreatic endocrine tumours. Clin Endocrinol 2008;68:271–7.
17. Database of Single Nucleotide Polymorphisms (dbSNP) [homepage on the Internet]. Bethesda (MD): National Center for Biotechnology Information, National Library of Medicine. Available from: <http://www.ncbi.nlm.nih.gov/SNP/>. Accessed 8/28/2014.
18. Roussel MF. The INK4 family of cell cycle inhibitors in cancer. Oncogene 1999;18:5311–7.
19. Wykoff CC, Sotiriou C, Cockman ME, Ratcliffe PJ, Maxwell P, Liu E, et al. Gene array of VHL mutation and hypoxia shows novel hypoxia-induced genes and that cyclin D1 is a VHL target gene. Br J Cancer 2004;90:1235–43.
20. Krimpenfort P, Ijpenberg A, Song J-Y, van der Valk M, Nawijn M, Zevenhoven J, et al. p15Ink4b is a critical tumour suppressor in the absence of p16Ink4a. Nature 2007;448:943–6.
21. Boultwood J, Wainscoat JS. Gene silencing by DNA methylation in haematological malignancies. Br J Haematol 2007;138:3–11.
22. Girgis AH, Iakovlev VV, Beheshti B, Bayani J, Squire JA, Bui A, et al. Multilevel whole-genome analysis reveals candidate biomarkers in clear cell renal cell carcinoma. Cancer Res 2012;72:5273–84.
23. Agarwal SK, Mateo CM, Marx SJ. Rare germline mutations in cyclin-dependent kinase inhibitor genes in multiple endocrine neoplasia type 1 and related states. J Clin Endocrinol Metab 2009;94:1826–34.
24. Castro-Vega LJ, Buffet A, De Cubas AA, Cascón A, Menara M, Khalifa E, et al. Germline mutations in FH confer predisposition to malignant pheochromocytomas and paragangliomas. Hum Mol Genet 2014;23:2440–6.
25. Clark GR, Sciacovelli M, Gaude E, Walsh DM, Kirby G, Simpson MA, et al. Germline FH mutations presenting with pheochromocytoma. J Clin Endocrinol Metab 2014;99:E2046–50.
26. Carpten JD, Robbins CM, Villablanca A, Forsberg L, Presciuttini S, Bailey-Wilson J, et al. HRPT2, encoding parafibromin, is mutated in hyperparathyroidism-jaw tumor syndrome. Nat Genet 2002;32:676–80.
27. Yang YJ, Han JW, Youn HD, Cho EJ. The tumor suppressor, parafibromin, mediates histone H3 K9 methylation for cyclin D1 repression. Nucleic Acids Res 2010;38:382–90.
28. Walsh DM, Shalev SA, Simpson MA, Morgan NV, Gelman-Kohan Z, Chemke J, et al. Acrocallosal syndrome: identification of a novel KIF7 mutation and evidence for oligogenic inheritance. Eur J Med Genet 2013;56:39–42.
29. Quinlan AR, Hall IM. BEDTools: a flexible suite of utilities for comparing genomic features. Bioinformatics 2010;26:841–2
30. Li H, Handsaker B, Wysoker A, Fennell T, Ruan J, Homer N, et al. The Sequence Alignment/Map format and SAMtools. Bioinformatics 2009;25:2078–9.
31. Wang K, Li M, Hakonarson H. ANNOVAR: functional annotation of genetic variants from high-throughput sequencing data. Nucleic Acids Res 2010;38:e164.
32. Morris MR, Hughes DJ, Tian YM, Ricketts CJ, Lau KW, Gentle D, et al. Mutation analysis of hypoxia-inducible factors HIF1A and HIF2A in renal cell carcinoma. Anticancer Res 2009;29:4337–43.
33. Sali A, Blundell TL. Comparative protein modelling by satisfaction of spatial restraints. J Mol Biol 1993;234:779–815.
34. Yuan C, Li J, Selby TL, Byeon IJ, Tsai MD. Tumor suppressor INK4: comparisons of conformational properties between p16(INK4A) and p18(INK4C). J Mol Biol 1999;294:201–11.
35. Pires DE, Ascher DB, Blundell TL. mCSM: predicting the effects of mutations in proteins using graph-based signatures. Bioinformatics 2014;30:335–42.
36. Pires DE, Ascher DB, Blundell TL. DUET: a server for predicting effects of mutations on protein stability using an integrated computational approach. Nucleic Acid Res 2014;42:W314–9.

AACR American Association for Cancer Research

CANCER DISCOVERY

Germline Mutations in the *CDKN2B* Tumor Suppressor Gene Predispose to Renal Cell Carcinoma

Mariam Jafri, Naomi C. Wake, David B. Ascher, et al.

Cancer Discovery 2015;5:723-729. Published OnlineFirst April 14, 2015.